VIP Nanoporous Membranes Very Important Paper

Deutsche Ausgabe: DOI: 10.1002/ange.201504838
Internationale Ausgabe: DOI: 10.1002/anie.201504838

# Highly Ordered Nanoporous Films from Supramolecular Diblock Copolymers with Hydrogen-Bonding Junctions

*Damien Montarnal, Nicolas Delbosc, Cécile Chamignon, Marie-Alice Virolleaud, Yingdong Luo, Craig J. Hawker, Eric Drockenmuller, and Julien Bernard**

***Abstract:*** *We designed efficient precursors that combine complementary associative groups with exceptional binding affinities and thiocarbonylthio moieties enabling precise RAFT polymerization. Well defined PS and PMMA supramolecular polymers with molecular weights up to 30 kg mol$^{-1}$ are synthesized and shown to form highly stable supramolecular diblock copolymers (BCPs) when mixed, in non-polar solvents or in the bulk. Hierarchical self-assembly of such supramolecular BCPs by thermal annealing affords morphologies with excellent lateral order, comparable to features expected from covalent diblock copolymer analogues. Simple washing of the resulting materials with protic solvents disrupts the supramolecular association and selectively dissolves one polymer, affording a straightforward process for preparing well-ordered nanoporous materials without resorting to cross-linking or invasive chemical degradations.*

Supramolecular assembly through non-covalent interactions has become an essential tool in the design of smart[1,2] and adaptive[3,4] materials, such as stimuli-responsive materials, gels capable of molecular-recognition,[5] or self-healing networks.[6,7] Mimicking the self-assembly of conventional diblock copolymers by hierarchical assembly of immiscible homopolymers with reversibly binding chain ends offers significant flexibility in the design and the processing of nanostructured materials. The two immiscible components can be prepared independently and are mixed without resorting to chemical coupling. Furthermore, the possibility to tune the strength of the supramolecular bond with various stimuli (e.g. temperature or solvent) enables dynamic properties such as micro or macro phase transitions. Supramolecular-mediated generation of ordered structures, such as nanoporous materials, could also be simplified and applied to prepare sensitive materials, such as biopolymers, low bandgap polymers, or ionic conductors. In contrast to classical methods requiring the degradation of sacrificial domains by invasive techniques (e.g. UV irradiation,[8] reactive ion[9] or chemical etching,[10] ozonolysis,[11] pyrolysis[12]) supramolecular coupling driven by strong H-bonding interactions allows one phase to be selectively dissolved by a solvent mixture with the adequate balance of polarity and selectivity.

The design of supramolecular diblock copolymers capable of assembly and high fidelity nanoscale pattern formation is a complex challenge with dispersive forces driving the incompatible homopolymers to phase separate on the macroscale. As a result, strong and directional binding interactions are required to maintain the interfacial junction and confine the phase separation to the scale of the polymer chains. Theoretical models describe phase diagrams of such systems by varying the segregation strength and the bond energy of the junction.[13,14] Notable achievements have taken place in this field since 2008[15–21] with strongly associating pairs, such as ureiodopyrimidinone (Upy) and diamidonaphtyridine (Napy), or guanosine and Napy groups, shown to promote compatibilization[22] or nanostructuration[23,24] of immiscible homopolymers. However, important bottlenecks remain to extend the scope of supramolecular diblock copolymer systems. The production of highly ordered morphologies like those observed for well-defined covalent diblock copolymers is still hampered by the difficulty to obtain quantitative chain-end functionalization for high molar mass building blocks (preparation of supramolecular block copolymers with molecular weights above 20 kg mol$^{-1}$ is indeed preferable to enforce microphase separation). Also, high thermal stability of the supramolecular complex is an essential requisite to achieve long-range ordering by thermal annealing.

Classic covalent PS-*b*-PMMA diblock copolymers (PS = polystrene; PMMA = poly(methyl methacrylate)) have been thoroughly studied over the last 20 years[25–27] (their self-assembly in bulk and in thin films being an excellent model system) and are still the preferred system for nanolithography in the microelectronics and data-storage technologies. However, their relatively low Flory–Huggins parameter ($\chi < 0.03$) requires high molecular weights for the copolymers to self-assemble into ordered morphologies ($M_n > 35$ kg mol$^{-1}$). Precise synthesis and self-assembly of such supramolecular analogues remain up-to-now untried and thus they constitute an ideal system to investigate the potential of supramolecular block copolymers.

To ideally mimic the self-assembly behavior of covalent PS-*b*-PMMA block copolymers, we took inspiration from Gong and co-workers (Figure 1),[28–30] who developed a re-

[*] Dr. D. Montarnal, Dr. N. Delbosc, C. Chamignon, Dr. M. A. Virolleaud, Prof. E. Drockenmuller, Dr. J. Bernard
Laboratoire d'Ingénierie des Matériaux Polymères (UMR CNRS 5223) Institut National des Sciences Appliquées (INSA-Lyon)—Université Lyon 1
17 av. Jean Capelle, 69621 Villeurbanne (France)
E-mail: julien.bernard@insa-lyon.fr
Y. Luo, Prof. C. J. Hawker
Materials Research Laboratory, University of Santa Barbara (USA)

Supporting information for this article (synthesis and characterization of supramolecular RAFT agents and polymers by SEC and $^1$H NMR, study of the self-assembly in dilute solution (SEC, DOSY NMR, ITC) and in the bulk (SAXS). Preparation of thin films and porous membranes and their observation with AFM and TEM) is available on the WWW under http://dx.doi.org/10.1002/anie.201504838.

  

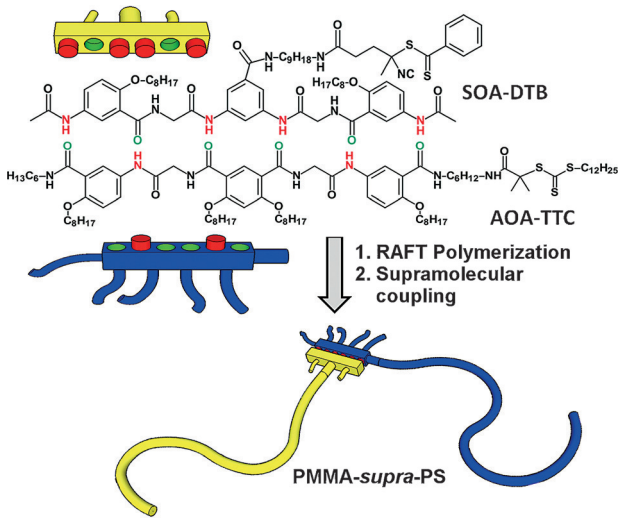


***Figure 1.*** RAFT agents functionalized with complementary symmetrical and asymmetrical donor–acceptor building blocks (SOA and AOA) enable the synthesis of well-defined supramolecular diblock copolymers from PMMA-SOA and PS-AOA H-bonding building blocks.

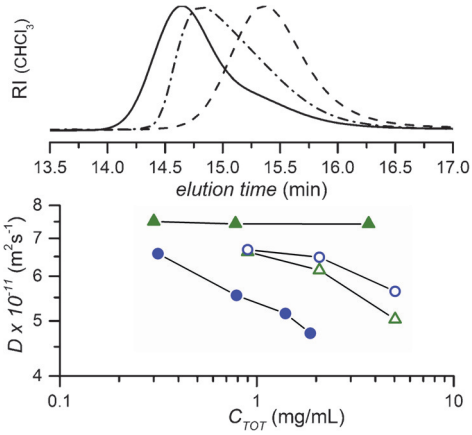


***Figure 2.*** Top: $CHCl_3$ SEC traces (RI signal) of $PS_{30k}$-AOA (dashed line), $PMMA_{30k}$-SOA (dashed-dotted line) and a 1:1 molar mixture (solid line), at concentrations of approximately 3 mg mL$^{-1}$. Bottom: Diffusion coefficients associated respectively to PMMA and PS signals for separately dissolved $PMMA_{30k}$-SOA (solid circles) and $PS_{30k}$-AOA (solid triangles) in $CDCl_3$ and when mixing both polymers in 1:1 molar ratio in $CDCl_3$ (open circles and open triangles, respectively). $C_{TOT}$ is the total concentration of species in solution.

markable pair of hetero-complementary building blocks exhibiting an extremely high association constant in chloroform ($CHCl_3$). Hydrogen-bonding reversible addition fragmentation chain transfer (RAFT) transfer agents based on the symmetrical oligoamide (SOA) and asymmetrical oligoamide (AOA) building blocks, see Figure 1, were therefore prepared through coupling reactions with *N*-hydroxysuccinimide ester functionalized dithiobenzoate (DTB) and trithiocarbonate (TTC), respectively. Long alkyl spacers were intercalated between the associating motifs and the mediating agents (DTB or TTC) to ensure both good solubility in organic solvents and decreased steric interactions for the thiocarbonylthio mediating and complementary associating groups during polymerization and subsequent hydrogen-bonding interactions. Amides were preferred over esters as links to impart chemical and thermal stability to the polymers. Details of the syntheses are given in the Supporting Information (Scheme S1 and S2). Polymerizations of MMA and styrene (mediated by SOA and AOA, respectively) were carried out at low AIBN:RAFT agent ratios (about 1:20; AIBN = 2,2′-azobis[(2-methyl)propanenitrile]) and moderate temperature (80 °C) to limit the formation of non-functionalized polymers chains from AIBN initiation. To yield supramolecular block copolymers with weight ratios around 50:50 and 66:33, two series of H-bonding PS and PMMA homopolymers with molecular weights of approximately 15 kg mol$^{-1}$ and 30 kg mol$^{-1}$ were synthesized ($PS_{30k}$-AOA, $M_{n\,SEC/THF} = 32.5$ kg mol$^{-1}$, $Đ = 1.15$, $PS_{15k}$-AOA, $M_{n\,SEC/THF} = 15.5$ kg mol$^{-1}$ $Đ = 1.13$; $PMMA_{30k}$-SOA, $M_{n\,SEC/THF} = 30.5$ kg mol$^{-1}$, $Đ = 1.14$; $PMMA_{15k}$-SOA, $M_{n\,SEC/THF} = 15.2$ kg mol$^{-1}$, $Đ = 1.13$).

The behavior of supramolecular polymers $PMMA_{30K}$-SOA and $PS_{30K}$-AOA and the formation of supramolecular diblock copolymers with 1:1 molar ratio of $PMMA_{30K}$-SOA and $PS_{30K}$-AOA were primarily studied in THF and $CHCl_3$ solutions (Figure 2). It is interesting to note that while $PS_{30k}$-AOA presents similar narrow traces in size exclusion chromatography (SEC) using THF or $CHCl_3$, the SEC trace of $PMMA_{30k}$-SOA is narrow and well defined using THF as eluent but significantly shifted and broadened in $CHCl_3$ thus suggesting H-bonding dimerization in less polar solvents as observed earlier by Gong et al.[31]

When using THF as a solvent, SEC traces of the two homopolymers superimpose with the trace of the mixture and no supramolecular diblock copolymer is observed (Figure S2).In direct contrast, SEC analysis of the 1:1 molar ratio $PMMA_{30K}$-SOA and $PS_{30K}$-AOA in $CHCl_3$, a less-polar solvent, reveals a clear shift of the SEC peak towards higher molecular weight ($V_e = 14.6$ mL, $M_{peak} \approx 60$ kg mol$^{-1}$, PS calibration) indicative of an efficient supramolecular coupling and the formation of the targeted supramolecular diblock copolymer. The unexpected stability of the supramolecular complex during the course of the SEC experiment (20+ minutes) is significant and illustrates the enhanced assembly driven by the AOA and SOA units. The tail observed at $V_e =$ 15.5 mL is attributed to the presence of homopolymers arising from minor deviations from stoichiometry. Besides, the presence of unfunctionalized PS and PMMA homopolymers cannot be undoubtedly discarded.

The solution behavior of the H-bonding PS and PMMA homopolymers and formation of supramolecular diblock copolymers were further investigated in dilute $CDCl_3$ solutions through diffusion ordered (DOSY) NMR spectroscopy (Figure S3, S4 and S2, experimental details in Supporting Information).[32,33] Consistent with the SEC analyses, the diffusion coefficients ($D$) of $PMMA_{30k}$-SOA in $CDCl_3$ were significantly lower than the ones measured for non-functionalized PMMA standards of equivalent molecular weight (30 kg mol$^{-1}$, $Đ = 1.04$). For the $PMMA_{30k}$-SOA block, $D$ showed a strong dependence on the concentration, and formation of aggregates was found down to 0.3 mg mL$^{-1}$,

that is, with [$PMMA_{30k}$-SOA] as low as 10 μmol $L^{-1}$. In contrast, $PS_{30k}$-AOA displays no variations of $D$ with concentration and no aggregation is found up to 10 mg $mL^{-1}$. When $PMMA_{30k}$-SOA and $PS_{30k}$-AOA are mixed in 1:1 molar ratio, both blocks show similar diffusion coefficients and diffuse together as a single object (Figure 2).

Isothermal calorimetry experiments (nanoITC) were then performed to characterize the thermodynamic parameters of the association between complementary blocks in anhydrous $CHCl_3$ solutions (Figure 3, experimental details given in Supporting Information). A dilute solution of $PS_{30k}$-AOA was titrated by successive injections of a concentrated solution of $PMMA_{30k}$-SOA. The enthalpogram shows a very sharp heat rate transition between the 9th and 10th injection, when the stoichiometry is reached, revealing very strong binding with further analysis of the heat exchanged during the titration confirming that a pairwise association occurs between the two blocks, with a binding constant about $K_a = 3.3 \times 10^7$ L $mol^{-1}$.

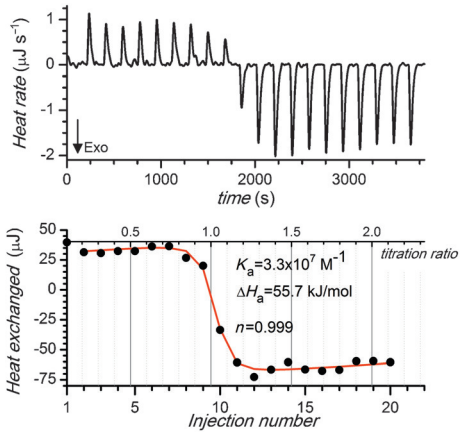


***Figure 3.*** Top: Enthalpogram of nanoITC titration in $CHCl_3$ ($PS_{30k}$-AOA, $c = 19$ μM titrated by $PMMA_{30k}$-SOA, $c = 399$μM; the arrow pointing down refers to exothermic events). Bottom: Estimation of binding parameters by fitting the heat exchanged during titration. The titration ratio (top scale) is the molar ratio between total injected amount of $PMMA_{30k}$-SOA and initial amount of $PS_{30k}$-AOA

The strength and efficiency of the supramolecular coupling demonstrated in solution is expected to promote nanostructure formation in the bulk in direct analogy with the phase-separated ordered morphologies observed for similar covalent diblock copolymers. Yet this hierarchical self-assembly is considerably more challenging as the entropic cost of coupling incompatible blocks is much higher in the absence of solvent. SAXS experiments were performed to assess the morphologies adopted by different blends of H-bonding polymers (Figure 4). The $PS_{30k}$-SOA/$PMMA_{30k}$-AOA blend shows a main scattering peak at $q_0 = 0.142$ $nm^{-1}$ corresponding to a domain spacing of 44 nm, that is, close to the 38 nm expected from the corresponding well-defined covalent diblock copolymers $PS_{30k}$-*b*-$PMMA_{30k}$.[34] The presence of higher order peaks with $q/q_0 = 2,3,4$, and 5, and lower intensities for even harmonics ($q/q_0 = 2$ and 4) is indicative of

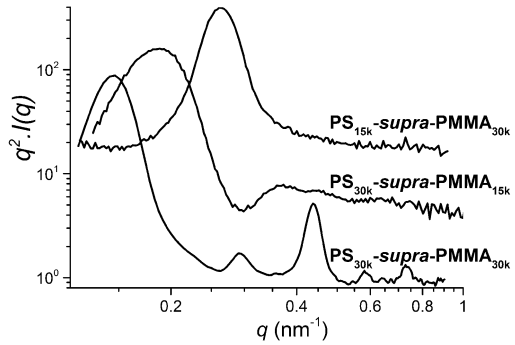


***Figure 4.*** Lorentz-corrected SAXS spectra of blends of supramolecular diblock copolymers. Traces are shifted vertically for clarity.

a well segregated symmetric lamellar morphology and demonstrate a clear hierarchical self-assembly of the supramolecular diblock referred thereafter as $PS_{30k}$-*supra*-$PMMA_{30k}$. The SAXS spectrum of the $PS_{30k}$-SOA/$PMMA_{15k}$-AOA blend also shows several harmonics characteristics of an ordered morphology, with a domain spacing of 34 nm (31 nm expected from monodisperse $PS_{30k}$-*b*-$PMMA_{15k}$). In contrast, the $PS_{15k}$-SOA/$PMMA_{30k}$-AOA blend shows no harmonic and a correlation length of 24 nm, a distance which is too small to be compatible with phase separation between PS and PMMA domains (32 nm expected from monodisperse $PS_{15k}$-*b*-$PMMA_{30k}$).

The utility of supramolecular self-assembly was further demonstrated by the preparation of thin films with nanoscale morphology and porosity. Silicon wafers were initially pretreated with a neutral layer of cross-linkable benzocyclobutene-based PS-*r*-PMMA copolymer to reduce preferential wetting on the substrate and promote a vertical alignment of the cylindrical features across the thin film.[35] The 60 nm-thick films of different combinations of supramolecular homopolymers were then spin-cast from toluene solutions and tapping-mode AFM images were taken after annealing the samples for 1 h at 180 °C (Figure 5 and Figures S6 and S7). $PS_{30k}$-*supra*-$PMMA_{15k}$ forms a very well ordered hexagonal lattice with a periodicity of approximately 39 nm and 17 nm wide domains (vertically oriented cylinders, see text below and Figures S6, S8, and S9) as would be expected for the covalent analogue. Under similar annealing conditions, $PS_{30k}$-*supra*-$PMMA_{30k}$ self-assembles into an unusual morphology: the lamellar structure with around 45 nm periodicity indicated by small-angle X-ray scattering (SAXS) is effectively visible, but the PMMA domains (in white on the phase pictures, Figure 5) are broken into approximately 30 nm spheres or cylinders. In contrast, the $PS_{15k}$-*supra*-$PMMA_{30k}$ film displays weak heterogeneities without clear phase separation or ordered morphology (Figure 5).

The observed difference in self-assembly behavior between $PS_{30k}$-*supra*-$PMMA_{15k}$ and $PS_{15k}$-*supra*-$PMMA_{30k}$ block copolymer systems is striking, and illustrates the dramatic influence of the asymmetric supramolecular junction. The oligoamide strand SOA attached to the PMMA homopolymer is less bulky that the AOA strand attached to PS. As a result, the interface curvature would favor PMMA spheres or cylinders and strong frustration is present when

  

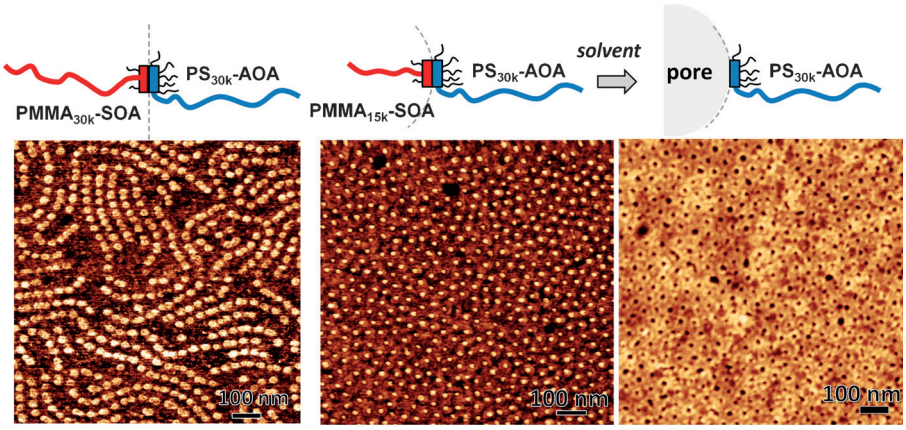


***Figure 5.*** Left and middle: AFM phase images of $PS_{30k}$-*supra*-$PMMA_{30k}$ and $PS_{30k}$-*supra*-$PMMA_{15k}$ thin films after 1 h annealing at 180°C. Right: AFM height image of $PS_{30k}$-*supra*-$PMMA_{15k}$ after immersion for 10 min in MeOH/$H_2O$/$CHCl_3$ (47.5:47.5:3). Top: schematic representation of the packing at the interface with the asymmetrical supramolecular junction, the dashed line shows the surface curvature imposed by the volume ratio of the blocks.

curvatures imposed by the supramolecular junction and the packing of polymer segments are contradictory. The formation of lamellae for $PS_{30k}$-*supra*-$PMMA_{30k}$ could be accommodated by small changes in packing for the PMMA domains, however the formation of PS cylinders for $PS_{15k}$-*supra*-$PMMA_{30k}$ is unfavorable. In contrast, for the $PS_{30k}$-*supra*-$PMMA_{15k}$ system, the supramolecular junction and the volume ratio of blocks, work together with self-assembly being favored. A similar although weaker effect has been reported for miktoarm block copolymers.[36]

We were also able to monitor in situ the thermal annealing of this sample using high-temperature AFM (Video in the Supporting Information, sequential images were obtained every 9 min after +5 °C increments). Sufficient mobility to initiate fluctuation and coarsening of the morphology was reached at 125 °C, and the formation of vertical cylinders starts as low as 150 °C with long-range ordering being obtained within minutes by isothermal annealing at 175 °C. Importantly, the resulting morphologies are stable even above 200 °C demonstrating the high thermal stability of the supramolecular complex.

The reversibility of supramolecular interactions also opens a new and versatile route for the generation of nanoporous materials. In contrast to covalent diblocks, in which sacrificial domains must first be degraded or the junction between blocks cleaved[37] with invasive treatments, polar solvents allow for facile disruption of supramolecular interactions. To demonstrate this ability, cylinder-forming $PS_{30k}$-*supra*-$PMMA_{15k}$ thin films were immersed for 10 min in mixed solvent systems. Pure $H_2O$/MeOH mixtures induce swelling of the PMMA domains (Figure S8), but offer insufficient solubility for PMMA-SOA to quantitatively desorb from the surface. When 10 wt% of $CHCl_3$ is added to enhance the removal of PMMA chains, the PS domains also swell and the nanostructure disappears. Conditions for the generation of nanopores are finally met when 3 wt% of $CHCl_3$ are added to the water/alcohol solution. Then well-ordered nanoporous films with pore diameters about 14 nm are observed (Figure 5). TEM imaging of these porous films lifted off from the substrates confirms the vertical orientation of the pores throughout the thin film (Figure S9).

The design of RAFT agents bearing hetero-complementary supramolecular groups with exceptional binding affinity introduces a new toolbox for obtaining high molecular weight supramolecular diblock copolymers that can undergo hierarchical self-assembly into stable well-ordered morphologies. By molecular design, important new features are introduced into supramolecular diblock copolymer systems leading to improved self-assembly through annealing. The reversibility inherent in these materials allows for the convenient generation of nanoporous membranes. This last characteristic is particularly useful for the assembly of sensitive polymers that are unable to withstand UV-light, heat, or other degradative techniques for domain removal in traditional block copolymer lithographic strategies.

## Acknowledgements

This work was supported by the Agence Nationale de la Recherche (Programme Blanc JCJC NAMASTE ANR-12-JS08-0011) and by the MRSEC program of the National Science Foundation (DMR 1121053, Y.L. and C.J.H.). Jean-Pierre Pascault is gratefully acknowledged for stimulating discussions and unwavering support. We are also indebted to Agnès Crépet for carrying out SEC experiments.

**Keywords:** hydrogen bonding · nanoporous membranes · RAFT agents · supramolecular diblock copolymers

**How to cite:** *Angew. Chem. Int. Ed.* **2015**, *54*, 11117–11121
*Angew. Chem.* **2015**, *127*, 11269–11273

[1] J. S. Moore, *Curr. Opin. Colloid Interface Sci.* **1999**, *4*, 108–116.
[2] L. Brunsveld, B. Folmer, E. Meijer, R. Sijbesma, *Chem. Rev.* **2001**, *101*, 4071–4098.
[3] J.-M. Lehn, *Prog. Polym. Sci.* **2005**, *30*, 814–831.
[4] T. Aida, E. Meijer, S. Stupp, *Science* **2012**, *335*, 813–817.
[5] A. Harada, R. Kobayashi, Y. Takashima, A. Hashidzume, H. Yamaguchi, *Nat. Chem.* **2011**, *3*, 34–37.
[6] P. Cordier, F. Tournilhac, C. Soulié-Ziakovic, L. Leibler, *Nature* **2008**, *451*, 977–980.
[7] H. Chen, X. Ma, S. Wu, H. Tian, *Angew. Chem. Int. Ed.* **2014**, *53*, 14149–14152; *Angew. Chem.* **2014**, *126*, 14373–14376.
[8] J. Bang, S. H. Kim, E. Drockenmuller, M. J. Misner, T. P. Russell, C. J. Hawker, *J. Am. Chem. Soc.* **2006**, *128*, 7622–7629.
[9] R. Olayo-Valles, M. S. Lund, C. Leighton, M. A. Hillmyer, *J. Mater. Chem.* **2004**, *14*, 2729–2731.

[10] C. Cummins, P. Mokarian-Tabari, J. D. Holmes, M. A. Morris, *J. Appl. Polym. Sci.* **2014**, *131*, 40795.
[11] J. S. Lee, A. Hirao, S. Nakahama, *Macromolecules* **1988**, *21*, 274 – 276.
[12] P. R. L. Malenfant, J. Wan, S. T. Taylor, M. Manoharan, *Nat. Nanotechnol.* **2007**, *2*, 43 – 46.
[13] Z. Mester, N. A. Lynd, K. T. Delaney, G. H. Fredrickson, *Macromolecules* **2014**, *47*, 1865 – 1874.
[14] E. H. Feng, W. B. Lee, G. H. Fredrickson, *Macromolecules* **2007**, *40*, 693 – 702.
[15] A. Bertrand, F. Lortie, J. Bernard, *Macromol. Rapid Commun.* **2012**, *33*, 2062 – 2091.
[16] W. H. Binder, S. Bernstorff, C. Kluger, L. Petraru, M. J. Kunz, *Adv. Mater.* **2005**, *17*, 2824 – 2828.
[17] M. C. Stuparu, A. Khan, C. J. Hawker, *Polym. Chem.* **2012**, *3*, 3033 – 3044.
[18] C.-A. Fustin, P. Guillet, U. S. Schubert, J.-F. Gohy, *Adv. Mater.* **2007**, *19*, 1665 – 1673.
[19] U. Rauwald, O. A. Scherman, *Angew. Chem. Int. Ed.* **2008**, *47*, 3950 – 3953; *Angew. Chem.* **2008**, *120*, 4014 – 4017.
[20] E. Weiss, K. C. Daoulas, M. Müller, R. Shenhar, *Macromolecules* **2011**, *44*, 9773 – 9781.
[21] O. Altintas, D. Schulze-Suenninghausen, B. Luy, C. Barner-Kowollik, *ACS Macro Lett.* **2013**, *2*, 211 – 216.
[22] K. E. Feldman, M. J. Kade, T. F. de Greef, E. Meijer, E. J. Kramer, C. J. Hawker, *Macromolecules* **2008**, *41*, 4694 – 4700.
[23] J. Rao, E. Paunescu, M. Mirmohades, I. Gadwal, A. Khaydarov, C. J. Hawker, J. Bang, A. Khan, *Polym. Chem.* **2012**, *3*, 2050 – 2056.
[24] L. M. Pitet, A. H. van Loon, E. J. Kramer, C. J. Hawker, E. Meijer, *ACS Macro Lett.* **2013**, *2*, 1006 – 1010.
[25] M. P. Stoykovich, P. F. Nealey, *Mater. Res. Materials Today* **2006**, *9*, 20 – 29.
[26] M. J. Fasolka, A. M. Mayes, *Annu. Rev. Mater. Res.* **2001**, *31*, 323 – 355.
[27] K. Koo, H. Ahn, S.-W. Kim, D. Y. Ryu, T. P. Russell, *Soft Matter* **2013**, *9*, 9059 – 9071.
[28] B. Gong, *Polym. Int.* **2007**, *56*, 436 – 443.
[29] H. Zeng, H. Ickes, R. A. Flowers, B. Gong, *J. Org. Chem.* **2001**, *66*, 3574 – 3583.
[30] X. Yang, F. Hua, K. Yamato, E. Ruckenstein, B. Gong, W. Kim, C. Y. Ryu, *Angew. Chem. Int. Ed.* **2004**, *43*, 6471 – 6474; *Angew. Chem.* **2004**, *116*, 6633 – 6636.
[31] H. Zeng, R. S. Miller, R. A. Flowers, B. Gong, *J. Am. Chem. Soc.* **2000**, *122*, 2635 – 2644.
[32] S. Viel, D. Capitani, L. Mannina, A. Segre, *Biomacromolecules* **2003**, *4*, 1843 – 1847.
[33] A. Jerschow, N. Müller, *Macromolecules* **1998**, *31*, 6573 – 6578.
[34] A. Mayes, T. Russell, S. Satija, C. Majkrzak, *Macromolecules* **1992**, *25*, 6523 – 6531.
[35] D. Y. Ryu, K. Shin, E. Drockenmuller, C. J. Hawker, T. P. Russell, *Science* **2005**, *308*, 236 – 239.
[36] W. Shi, N. A. Lynd, D. Montarnal, Y. Luo, G. H. Fredrickson, E. J. Kramer, C. Ntaras, A. Avgeropoulos, A. Hexemer, *Macromolecules* **2014**, *47*, 2037 – 2043.
[37] K. Satoh, J. E. Poelma, L. M. Campos, B. Stahl, C. J. Hawker, *Polym. Chem.* **2012**, *3*, 1890 – 1898.

Received: May 28, 2015
Published online: July 31, 2015

  